Science of the Total Environment 743 (2020) 140564

Contents lists available at ScienceDirect

Science of the Total Environment

journal homepage: www.elsevier.com/locate/scitotenv

Fish growth rates and lake sulphate explain variation in mercury levels in ninespine stickleback (*Pungitius pungitius*) on the Arctic Coastal Plain of Alaska

S.M. Burke [a,b,*], C.E. Zimmerman [c], S.M. Laske [c], J.C. Koch [c], A.M. Derry [d], S. Guernon [d], B.A. Branfireun [e], H.K. Swanson [a]

[a] Department of Biology and Water Institute, University of Waterloo, 200 University Ave. West, Waterloo, Ontario N2L 3G1, Canada
[b] Environment and Climate Change Canada (ECCC), Aquatic Contaminants Research Division, 867 Lakeshore Rd., Burlington, ON L7S 1A1, Canada
[c] U. S. Geological Survey, Alaska Science Center, 4210 University Dr., Anchorage, AK 99508, USA
[d] Département des sciences biologiques, Université du Québec à Montréal (UQAM), P.O. Box 8888, Succ. Centre-Ville, Montréal, Québec H3C 3P8, Canada
[e] Western University, Department of Biological Sciences, London, Ontario N6A 3K7, Canada

HIGHLIGHTS

- Catchment characteristics affected fish Hg in lakes on the Arctic Coastal Plain.
- Methylation sites (sediments vs periphyton) influenced MeHg in biota.
- Fish growth and water sulphate explained most among-lake variability in fish Hg.

GRAPHICAL ABSTRACT

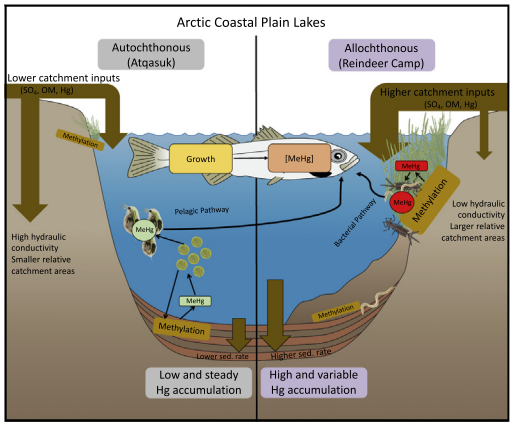

ARTICLE INFO

Article history:
Received 15 April 2020
Received in revised form 24 June 2020
Accepted 25 June 2020
Available online 2 July 2020

Editor: Mae Sexauer Gustin

Keywords:
Mercury
Arctic Coastal Plain
Ninespine stickleback
Methylation
Thermokarst lakes

ABSTRACT

Mercury concentrations in freshwater food webs are governed by complex biogeochemical and ecological interactions that spatially vary and are often mediated by climate. The Arctic Coastal Plain of Alaska (ACP) is a heterogeneous, lake-rich landscape where variability in mercury accumulation is poorly understood. Earlier research indicated that the level of catchment influence on lakes varied spatially on the ACP, and affected mercury accumulation in lake sediments. This work sought to determine drivers of spatial variation in mercury accumulation in lake food webs on the ACP. Three lakes that were a priori identified as "high catchment influence" (Reindeer Camp region) and three lakes that were a priori identified as "low catchment influence" (Atqasuk region) were sampled, and variability in water chemistry, food web ecology, and mercury accumulation was investigated. Among-lake differences in ninespine stickleback (*Pungitius pungitius*) length-adjusted methylmercury concentrations were significantly explained by sulphate concentration in lake water, a tracer of catchment runoff input. This effect was mediated by fish growth, which had no pattern between regions. Together, lake water sulphate concentration and fish age-at-size (proxy for growth) accounted for nearly all of the among-lake variability

* Corresponding author at: University of Waterloo, Canada.
E-mail address: samantha.burke2@gmail.com (S.M. Burke).

https://doi.org/10.1016/j.scitotenv.2020.140564

Sulphate
Catchment

in length-adjusted methylmercury concentrations in stickleback ($R^2_{adj} = 0.94$, $p < 0.01$). The percentage of total mercury as methylmercury (a proxy for net Hg methylation) was higher in sediments of more autochthonous, "low catchment influence" lakes ($p < 0.05$), and in the periphyton of more allochthonous, "high catchment influence" lakes ($p < 0.05$). The results indicate that dominant sources of primary production (littoral macrophyte/biofilm vs. pelagic phytoplankton) and food web structure (detrital vs. grazing) are regulated by catchment characteristics on the ACP, and that this ultimately influences the amount of methylmercury in the aquatic food web. These results have important implications for predicting future mercury concentrations in fish in lakes where fish growth rates and catchment inputs may change in response to a changing climate.

1. Introduction

Mercury (Hg) is a neurotoxin, and in its methylated form (methylmercury; MeHg), it bioaccumulates and biomagnifies in aquatic food webs (e.g., Kidd et al., 1995; Lockhart et al., 2005) to reach concentrations that are often high enough to affect the health of humans and fish-eating wildlife (e.g., Lockhart et al., 2005). Several interrelated physical, biogeochemical, and ecological variables influence methylation, uptake, and bioaccumulation of Hg in aquatic ecosystems and food webs. Ultimately, MeHg concentrations ([MeHg]) in fish are governed by the amount of available MeHg at the base of the food web, the rate of biomagnification through the food web, and the rate of accumulation in individual fish (see Lehnherr, 2014). The amount of MeHg available at the base of lake food webs is controlled by the amount of bioavailable inorganic Hg and the activity of methylators, which are typically sulphate-reducing bacteria (SRB; Compeau and Bartha, 1985), but can also be iron-reducing bacteria and/or methanogenic archaea (see Lehnherr, 2014). Multiple environmental variables interact to affect rates of mercury methylation by SRB, including concentrations of sulfate (SO_4; Gilmour et al., 1992) and dissolved organic matter (DOM; Graham et al., 2012). Elevated sulphate concentrations can stimulate SRB; however, there is an optimum above which sulphate can inhibit Hg methylation due to the production of sulfide (Gilmour et al., 1992). Similarly, DOM can stimulate SRB because microbes use it as an energy source (see Ravichandran, 2004), but at high concentrations DOM can inhibit Hg methylation through formation of Hg-DOM complexes (see Ravichandran, 2004; Paranjape and Hall, 2017).

While mercury methylation was originally described to primarily occur in lake sediment pore-waters (Korthals and Winfrey, 1987), it has also been found to occur in the water column (Watras et al., 1995; Mauro et al., 2002), in biofilm associated with macrophyte beds (e.g., Mauro et al., 2002; Achá et al., 2012), and in catchment wetlands (e.g., Bravo et al., 2017). Authors of a recent study on boreal lakes investigated effects of organic matter composition on mercury methylation rates and concentrations of MeHg in boreal lake sediments (Bravo et al., 2017). Overall, bacterial activity and Hg methylation rates were higher in sediments with higher concentrations of autochthonous (phytoplankton-derived) organic compounds. Lake sediments that were dominated by allochthonous (terrestrial-derived) organic compounds had lower Hg methylation rates, but higher overall MeHg concentration. The results suggested that allochthonous OM is less labile (bioavailable to methylators) than autochthonous OM, but that significant Hg methylation was occurring in lake catchments (Bravo et al., 2017).

Once methylated, uptake of Hg into lake food webs and accumulation in fish is influenced by fish growth rates (Karimi et al., 2007; Swanson and Kidd, 2010), age, condition (Scott and Armstrong, 1972; Sandheinrich and Drevnick, 2016), foraging habits (Kahilainen et al., 2016), and trophic position (Kidd et al., 2012). Generally, Hg concentrations are higher in slower-growing (Karimi et al., 2007), older fish (Scott and Armstrong, 1972), and in fish that feed at higher trophic positions (e.g., Kidd et al., 2012). Primary production can also influence Hg uptake into food webs (Pickhardt et al., 2002; Ahonen et al., 2018), through effects on growth and feeding ecology of fish (Kahilainen et al., 2016). While high pelagic primary production can lead to greater scavenging of Hg from the water column (Outridge et al., 2007) and higher Hg methylation rates, high primary production can also decrease the amount of MeHg entering the food web through bloom dilution (Pickhardt et al., 2002).

Many of the factors that affect mercury methylation, uptake, and bioaccumulation are subject to effects of climate change, but the net effects of climate change on mercury levels in Arctic aquatic ecosystems are difficult to predict. For example, climate-induced increases in lake primary production may act to either increase or decrease fish Hg concentrations via stimulation of microbial mercury methylation, or increased fish growth rates, respectively. Thermokarst processes are also increasing in frequency and magnitude with rising air temperatures (see Grosse et al., 2013), and can act to increase or decrease Hg accumulation, depending on the composition and chemistry of materials and solutes that are released (e.g., Kokelj et al., 2009; Deison et al., 2012). Permafrost thaw on the Arctic coastal plain delivers solutes and nutrients to water bodies, and affects biogeochemical and microbial processes (Koch et al., 2018a,b) that likely regulate mercury methylation.

Mercury is primarily delivered to Arctic lakes and catchments via the atmosphere. Although anthropogenic emissions of Hg to the atmosphere are declining due to emissions controls (see AMAP, 2011), there is a large amount of mercury stored in permafrost soils that can be remobilized with permafrost thaw (Schuster et al., 2018). Currently, there is a paucity of biotic mercury data for the Arctic Coastal Plain of Alaska (ACP), a lake-rich region in northern Alaska that stretches from the foothills of the Brooks Range (68°N) to the Beaufort and Chukchi Seas (71°N) (AMAP, 2011). To our knowledge, abiotic and biotic predictors of fish mercury levels in ACP lakes have not been explicitly investigated. It is evident, however, that current fish mercury levels in ACP lakes can negatively affect the health of fish-eating wildlife, such as loons (Scheuhammer et al., 2008; Evers et al., 2014). In a previous study, Burke et al. (2018) found regionally variable mercury accumulation in the sediments of thermokarst lakes on the ACP. Sediment Hg accumulation rates were high and variable in lakes found in the Reindeer Camp region of the ACP (Burke et al., 2018). Catchments in this region had lower hydraulic conductivity and higher runoff potential (Koch, 2020), and lakes were thus categorized as "high catchment influence." In contrast, sediment Hg accumulation rates in the Atqasuk region of the ACP were relatively lower and more temporally consistent (Burke et al., 2018), catchments had higher hydraulic conductivities (Koch, 2020) and lower runoff potential, and lakes were thus categorized as "low catchment influence". In "low catchment influence" lakes, sediment Hg accumulation rates were driven by primary production (Burke et al., 2018). Because sedimentation events, as well as rates and sources of primary production and organic matter, can affect Hg methylation and bioaccumulation in fish, it is likely that Hg concentrations in food webs vary between the Atqasuk and Reindeer Camp regions on the ACP.

The objectives of this study were to:

1. Investigate differences in the chemistry of thermokarst lakes between two regions on the ACP that differ in their presumed relative degree of catchment influence and;

2. Determine how differences in lake chemistry (with some measures acting as proxies for catchment influence), and among-lake differences in ecology, affect [MeHg] in sediment, periphyton, zooplankton, macroinvertebrates, and fish. It was hypothesized that lakes with relatively high inferred catchment influence would have different chemistry than lakes with relatively low inferred catchment influence, and that this would be reflected in differences in fish mercury concentrations. It was predicted that the water chemistry of lakes within inferred relatively high catchment influence would reflect greater allochthonous inputs of dissolved inorganic carbon and ions (reflective of catchment mineral weathering; Petrone et al., 2006; Koch et al., 2018a,b), OM (higher Specific UV Absorbance at 254 nm (SUVA) a measure of carbon aromaticity and indicator or terrestrial influence; Frey et al., 2016), and Hg, and consequently higher Hg levels in biota. It was further expected that differences in Hg concentrations between regions and among lakes would be related to variables that indicate source and amount of primary production (e.g., chlorophyll-*a* (Chl-*a*), dissolved organic carbon, DOC; Bravo et al., 2017; Poste et al., 2019).

2. Methods

2.1. Study area

The six lakes included in this study are located on the Arctic Coastal Plain (ACP) of Alaska (Fig. 1), which extends north from the Brooks Range (68°N) to the Beaufort and Chukchi Seas (71°N). The lakes are located within a zone of continuous permafrost on tussock tundra, and two regions are represented by the selected lakes: the Atqasuk (ATQ) region (lakes: ATQ 200, ATQ 201, ATQ 206), and the Reindeer Camp (RDC) region (lakes: RDC 308, RDC 309, RDC 311). Three lakes at each region were selected using data from the Circumarctic Lakes Observation Network (CALON; Hinkel, 2013); water temperatures were collected from several lakes in each node from 2011 to 2015, and lakes were chosen based on feasibility of access (via float plane), and physical characteristics, such as depth, surface water connectivity, and presence of water under ice that were indicative of fish presence and relatively higher food web complexity (Haynes et al., 2014; Laske et al., 2019). The lakes are shallow (2–4 m), small (0.5–2.5 km^2), and well-mixed during the open water season (Hinkel, 2013) The food webs of ACP lakes are relatively simple, and contain few fish species (e.g., Laske et al., 2019). The most common fish species are ninespine stickleback (*Pungitius pungitius*) and Alaska blackfish (*Dallia pectoralis*). The ACP is a heterogeneous landscape, and there are hydrological and other physical differences between the ATQ and RDC regions. Catchments in the ATQ region are characterized by sandy, well-drained soils with high hydraulic conductivity (Koch, 2020). Based on the previous work of Burke et al. (2018) and Koch (2020), these lakes were a priori classified as "lower catchment influence." Catchments in the RDC region are inferred to be larger relative to lake area than catchments in the ATQ region based on existing information (a previous study found >3 fold greater catchment: lake area ratio between an RDC and ATQ lake; Burke et al., 2018). Soils in the RDC region are silty with thick, organic-rich surface layers (Jorgenson and Grunblatt, 2013), and have lower hydraulic conductivity (Koch, 2020) than those in the ATQ region; this makes them prone to higher runoff. The RDC lakes were a priori classified as "higher catchment influence." To evaluate this a priori classification and in the absence of feasible catchment delineation (due to extremely low relief) and composition data, here several water chemistry variables (e.g., Cl, SO4, SUVA, Ca) are used as indicators of relative catchment influence; these variables integrate multiple catchment properties, including relative size and extent of runoff.

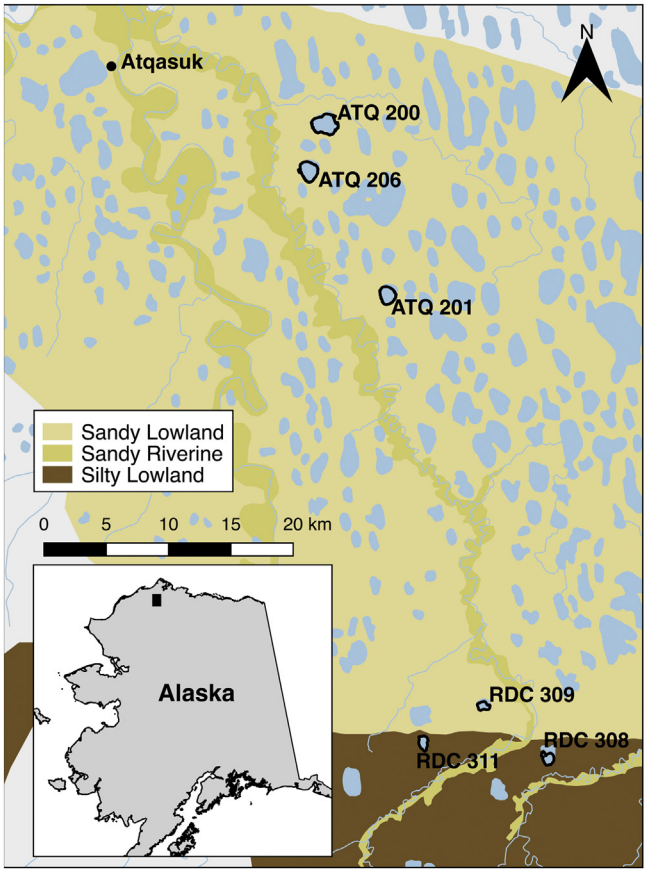

Fig. 1. A map of the study lakes on the Arctic Coastal Plain of Alaska (Atqasuk: ATQ 200, ATQ 201, ATQ 206; Reindeer Camp: RDC 308, RDC 309, RDC 311); black circle represents the community of Atqasuk.

2.2. Sample collection and preparation

During the period between July 25th and August 7th, 2016, a variety of biotic (i.e., fish, macroinvertebrates, zooplankton, macrophytes, periphyton/biofilm) and abiotic (i.e., water and sediment) samples were collected from each of the six study lakes. Fish were collected using fyke nets and minnow traps. Upon collection, fish were sacrificed, measured for total length (nearest mm) and weight (nearest centigram), and frozen whole at −20 °C for further processing and future analyses of stable isotope ratios and mercury concentrations. The only fish species collected from all lakes was ninespine stickleback. As such, further analyses focused on this species. Ninespine stickleback are a small freshwater fish species from the family Gasterosteidae that are found throughout the circum-Arctic, and primarily feed on zooplankton and dipteran larvae (Hynes, 1950). In a subset of lakes, other fish species were found including Arctic grayling (*Thymallus arcticus*; ATQ 200, ATQ 206) and Alaska blackfish (ATQ 206, RDC 309, RDC 311).

Primary consumers (benthic macroinvertebrates and zooplankton) were also collected from each lake. Benthic invertebrates were collected using dip nets (nearshore; 250 μm mesh) and an Ekman dredge (offshore; 250 μm mesh). After collection, macroinvertebrates were sorted, identified to taxonomic Family, and frozen at −20 °C for further processing and future analyses of stable isotope ratios and mercury concentrations. Nearshore and offshore samples were combined to generate sample masses that were adequate for laboratory analyses. Bulk zooplankton (i.e., bulk seston) samples were collected from the pelagic zone of each lake by pumping 60 L of water through 54 μm acid-washed (10% trace metal grade HCl) Nitex mesh. Samples were frozen at −20 °C for further processing and future analyses of stable isotope ratios and mercury concentrations.

All water samples were collected from the approximate centre of each lake for laboratory analyses of turbidity, and concentrations of

nutrients and ions. Surface water samples (1 L) were also collected in brown Nalgene bottles and filtered onshore (300–800 mL) using ethanol-rinsed 0.42 μm GF/F filters (then frozen at −20 °C) for analyses of Chl-*a*. Unfiltered water samples (250 mL) for Hg analysis were collected via a surface grab using the 'clean hands-dirty hands' technique (U.S. EPA, 1996). Filtered water samples (250 mL) for Hg analysis were collected by using a peristaltic pump and an acid-washed Teflon line that was deployed slightly below surface. Water samples were filtered through quartz QMA filters that had been muffled at 450 °C for 20 min and stored in acid-washed petri dishes. Filters were mounted in acid-washed re-usable cartridges. All water samples were preserved with ultra-trace hydrochloric acid at a concentration of 1% by volume. Following collection of filtered water for Hg analysis, the same filtering apparatus was used to collect samples for analyses of DOC and DIC (dissolved inorganic carbon). Filter lines and cartridges were changed between lakes.

Sediment samples were collected from the same approximate mid-lake location as water samples using an Ekman dredge. The top 2–3 cm of sediment was collected from the top opening of the dredge using an acid-washed Teflon spoon (care was taken to not sample sediments touching the sides). The sample was placed in a Whirl-pak™ bag before being frozen at −20 °C prior to further processing and analysis of mercury concentrations. Periphyton samples were collected by gloved-hand and acid-washed syringes from algal mats and macrophyte beds, and frozen prior to laboratory processing and stable isotope and mercury analyses. Periphyton was collected from both the surface of macrophytes and sediments; the samples analyzed represent a composite of available periphyton in the littoral zone of each lake. Percent cover of submerged macrophytes in the littoral zone of each lake was estimated visually (<10%, 10–25%, 25–50%, 50–75%, 75–90%, or 90–100%) during low-altitude flights that were conducted along the shoreline of each lake.

2.3. Laboratory analysis

All biological samples (fish, macroinvertebrates, zooplankton, periphyton) and sediment samples were freeze-dried using a LabConco FreeZone operated at −54 °C and 0.014 mBar for 48 h. Freeze-dried samples were ground to a uniform powder using acid-washed and Milli-Q®-rinsed scissors inside borosilicate scintillation vials. Prior to freeze-drying, whole stickleback had their otoliths and guts removed, and macroinvertebrates were sorted by family and removed from shells where applicable (i.e., mussels, snails). All further analyses on fish were completed on whole body samples (minus guts), as previous work by Swanson and Kidd (2010) indicated no difference in Hg concentrations between muscle and whole-body samples. Laboratory analyses were completed in compliance with cited methods, and QA/QC details are presented in the Supplemental information.

Analyses of methylmercury (MeHg) concentrations on fish, zooplankton, benthic macroinvertebrates, periphyton, and sediment were completed at the Biotron Analytical Services Laboratory at Western University, London, Ontario, Canada. Briefly, a potassium hydroxide solution (KOH) was added to sample tissues prior to hot block digestion (Bloom and Fitzgerald, 1988), and resulting extracts were speciated by gas chromatography and analyzed using cold vapor atomic fluorescence spectroscopy on a Tekran 2700 Automated MeHg Analysis System following U.S. EPA method 1630 (U.S. EPA, 1998). Ten to 15 mg of tissue from a subset (10%) of ninespine stickleback were analyzed for methylmercury whereas all macroinvertebrates, zooplankton, sediment, and periphyton samples were analyzed for methylmercury (see SI for QA/QC).

Total Hg analysis was completed on all fish, sediment, and periphyton samples, and on benthic macroinvertebrate and zooplankton samples that had enough mass for both methyl (first priority) and total mercury analyses. Total mercury analysis on fish (260 fish; mean = 44 ± 12 (s.d.)/lake) was completed at the University of Waterloo, Waterloo, Ontario, Canada, using an Ohio Lumex PYRO-915+ (100-240 V, 50/60 Hz, 700 W; Burger et al., 2004). Approximately 10–15 mg of dry tissue was used for THg analysis. Total mercury analysis on sediment and periphyton was conducted at the Biotron Analytical Services Laboratory using a Milestone DMA-80, for which the method detection limit was 0.714 ng/g (dry weight; see SI for QA/QC).

Analyses for stable carbon and nitrogen isotope ratios were completed on fish, macroinvertebrate, and zooplankton samples at the Environmental Isotope Laboratory at the University of Waterloo, Waterloo, Ontario. Stable isotope ratios are expressed as delta values ($\delta^{13}C$, $\delta^{15}N$) in parts per mil (‰) relative to international standards (Pee-Dee Belemnite and N_2 gas, respectively), and values presented are raw (i.e., not baseline-corrected see SI for QA/QC).

To estimate fish age, one sagittal otolith from each fish was submerged in water and photographed (Leica Application Suite version 4.0.0, Leica Microsystems [Switzerland] Limited) at 40× magnification under a dissecting microscope (Leica M60) at the USGS Alaska Science Center, Anchorage, Alaska. Two independent readers counted visible annuli under reflected light (Jones and Hynes, 1950; DeFaveri et al., 2014). If results from the two readers did not agree, a third reader provided an independent estimate (<7% of samples).

Water samples were analyzed for a suite of standard water chemistry parameters (e.g., nutrients, ions, dissolved organic carbon) at the University of Alberta Biogeochemical Analytical Service Laboratory in Edmonton, Alberta. Total and methylmercury analyses in water were completed at the Biotron Analytical Services Laboratory at Western University, London, Ontario, using a Tekran 2600 and 2700, respectively. To assess DOC quality and bioavailability, water samples were analyzed for SUVA (the UV absorbance at 254 nm, normalized for DOC concentration) using methods outlined in Weishaar et al. (2003) with a Spectramax® M2 spectrophotometer (Molecular Devices Corp., Sunnyvale, CA, USA) in the Watershed Hydrology Group Laboratory at McMaster University, Ontario, Canada.

2.4. Data analysis

All statistical analyses were completed using R Studio v 1.0.136 and R v 3.5.1 with core packages, as well as "lsmeans" (Lenth, 2016) and "vegan" (Oksanen et al., 2013) packages. G*Power v 3.1.9.6 (Faul et al., 2007) was used to conduct power analyses. Figures were generated using Sigmaplot v 11.0 (Systat, 2008) or QGIS version 2.16.3 (QGIS Development Team, 2016). As mentioned above, MeHg analyses were completed on a subsample of fish (10%) that were analyzed for total mercury. A mean ratio of [MeHg] to [THg] was calculated for the subset of stickleback in each lake, and since there was a significant difference in %MeHg of THg among lakes (ranging from 74 to 91%, see SI), the individual lake ratios were used to convert all of the THg concentrations in the remaining stickleback to estimated MeHg concentrations after it was determined there was no effect of length on the relationship between THg and MeHg (see SI, Table S1). Since the focus of this study is among-lake variation in MeHg, estimated MeHg concentrations were then used in all further data analyses. When data were not normally distributed, a $\log_e$ transformation was applied. Alpha was set to 0.05. Because the goal was to assess landscape-level drivers of fish mercury, lakes act as replicates in this study ($n = 6$). As such, many analyses were completed on single measures of variables from each lake (i.e., water chemistry, sediment, periphyton, zooplankton), means of pooled taxa (i.e., benthic macroinvertebrates), or on LSmeans (i.e., stickleback) estimated from multiple samples (see SI, Tables S2, S3 for further detail).

Results of water chemistry analyses were assessed with a principal components analysis, and Student's *t*-tests were used to compare a subset of variables (DOC: Chl-*a* ratios, THg, and MeHg) between regions. Student's *t*-tests were also used to compare mean [MeHg] in sediment, periphyton, zooplankton (bulk sample), and benthic macroinvertebrates between regions. Post-hoc power analyses were completed on each of the regional *t*-tests (Table S4).

Percent MeHg (of total Hg) in sediment and periphyton (the most likely locations of Hg methylation) was used as a proxy of net methylation rates, and Pearson's product-moment correlations and linear regressions were used to identify and model, respectively, relationships between % MeHg in periphyton and sediment and a subset of water chemistry variables across the study lakes (See Table S6, Supplemental information). To better understand the trophic ecology of each region, stable isotope biplots were created using mean ratios generated for fish, benthic macroinvertebrates, and zooplankton in each lake. Student's *t*-tests were used to compare taxa-specific mean $\delta^{15}N$ and $\delta^{13}C$ between regions.

Because mercury is known to increase with fish length (e.g., Bodaly et al., 1993; Swanson and Kidd, 2010), an analysis of covariance (ANCOVA) was used to generate least squares mean (LSmean; see SI; Swanson and Kidd, 2010; Swanson et al., 2011) [MeHg] at a standardized total length of 50 mm (mean total length, no extrapolation required) for stickleback from each lake. LSmean [MeHg] values were then compared between regions with a Student's *t*-test, and related to variables known to affect mercury bioaccumulation using Pearson product-moment correlations. Variables included in the correlation analysis were: fish age-at-size (generated using ANCOVA at a total length of 50 mm; see SI), fish $\delta^{15}N$, fish $\delta^{13}C$, SO_4, DIC, chloride (Cl), DOC, DOC:Chl-*a*, total nitrogen (TN), total phosphorus (TP), pH, turbidity, and Chl-*a*. Significant variables from these analyses were then included in a multiple regression. Collinearity was assessed using condition indices, tolerance values, and variance inflation factors. Residuals were examined following analyses to assure assumptions of each test (normal residuals, homogeneity of variance) were met.

3. Results and discussion

3.1. Lake water chemistry and inferred catchment connectivity

Lake water chemistry results showed that RDC lakes were more strongly influenced by allochthonous inputs than ATQ lakes. RDC lakes had higher concentrations of DIC, DOC, SO_4, Ca, and Cl (*t*-test; $t > 3.03$, $p < 0.05$, df = 4) than ATQ lakes (Table 1). SUVA was generally higher in the RDC lakes than in the ATQ lakes but the difference was not statistically significant (*t*-test; $t = 2.3$, $p = 0.08$, df = 4) likely due to low power (Table S4).

Often applied in the context of a mixing model to conduct source attribution of runoff (see Christophersen and Hooper, 1992 as a foundational work), elements that are derived from mineral weathering (e.g. Ca^{2+}, Mg^{2+}, K^+, Na^+) are indicators of waters with a catchment-like/groundwater geochemistry. In addition, DOC and specifically SUVA (a measure of the relative proportion of the higher molecular weight terrestrially-derived fraction of dissolved organic matter; e.g. Frey et al., 2016) can be used as tracers of catchment inputs (e.g., Petrone et al., 2006; Koch et al., 2018a,b). Principal components analysis clearly illustrated differences in water chemistry between regions (Fig. 2). Principal component 1 (PC1) explained 67% of the variability in water chemistry, and reflected a gradient of autochthony to allochthony (Fig. 2). Variables associated with terrestrial/catchment influence (DIC, DOC, Cl, SO_4, Ca, SUVA) had positive loadings on PC1 whereas indicators of higher autochthonous production (Chl-*a*, TP and turbidity) had negative loadings on PC1 (Fig. 2). ATQ lakes had significantly more negative PC1 scores than RDC lakes (*t*-test; $t = 4.96$, $p = 0.01$, df = 4; Fig. 2).

The higher catchment influence and greater allochthony in RDC lakes is consistent with previously reported data on catchment soils and hydrology from these regions, and supports the a priori classification. The ATQ lakes are located on sandy, well-drained soils with high hydraulic conductivity (Koch, 2020). In contrast, the RDC lakes likely have larger relative catchment sizes; a previous study found >3 fold greater catchment: lake area ratio between an RDC and ATQ lake (Burke et al., 2018). RDC lakes also have silty catchment soils with thick, organic-rich surface layers (Jorgenson and Grunblatt, 2013) that result in lower hydraulic conductivity (Koch, 2020).

Higher Chl-*a* concentrations (Table 1) and significantly lower DOC: Chl-*a* ratios further suggest that there is more autochthonous primary production in the ATQ lakes compared to the RDC lakes (*t*-test; $t = 3.83$, $p = 0.02$, df = 4; Rose et al., 2015). Based on these data and visual observations (aerial) of macrophyte cover (Table 1), we posit that differences in degree of catchment influence have led to phytoplankton dominance in the ATQ lakes, while in-lake production within RDC lakes is macrophyte-dominated. Studies have shown that in lakes with high sediment inputs, such as those with thermokarstic activity (Mesquita et al., 2010; Thienpont et al., 2013), primary production is often dominated by macrophytes. This occurs because water draining minerogenic soils is rich in ionic-organic compounds that precipitate from the water column once in lakes (Thompson et al., 2008; Kokelj et al., 2009), leading to greater water transparency and establishment of macrophytes (see Kalff, 2001).

Table 1
Select physical, chemical, and biological characteristics of the six study lakes (Atqasuk: ATQ 200, ATQ 201, ATQ 206; Reindeer Camp: RDC 308, RDC 309, RDC 311). Samples for all lakes were collected in summer 2016.

	ATQ 200	ATQ 201	ATQ 206	RDC 308	RDC 309	RDC 311
Latitude (decimal degrees)	70.453	70.327	70.416	69.987	70.025	69.995
Longitude (decimal degrees)	−156.953	−156.805	−156.981	−156.427	−156.567	−156.689
Surface area (km^2)	2.49	1.37	1.79	0.73	0.50	0.67
Zmax (m)	2.56	3.0	2.96	4.08	2.07	3.05
THg_{unfilt} (ng/L)	0.45	0.46	0.44	0.29	0.49	0.25
$MeHg_{unfilt}$ (ng/L)	0.026	0.022	0.012	0.015	0.015	0.015
pH	7.10	7.25	7.59	8.46	7.74	8.19
DOC (mg/L)	3.22	4.87	4.17	8.09	8.10	5.99
DIC (mg/L)	1.94	3.39	7.13	23.50	10.06	23.21
SO_4 (mg/L)	0.03	0.20	0.05	4.51	0.38	0.80
TN (μg/L)	367	367	378	407	440	331
TP (μg/L)	12	11	7	5	9	3
Cl (mg/L)	2.90	5.25	4.67	11.09	10.18	16.21
Ca (mg/L)	4.09	5.88	11.31	37.97	17.58	35.57
Chl-*a* (μg/L)	4.59	6.51	3.51	2.63	3.40	3.34
DOC:Chl-*a*	0.70	0.75	1.19	3.08	2.38	1.79
Turbidity (NTU)	0.73	0.51	0.62	0.58	0.62	0.18
SUVA	1.34	0.89	1.28	2.01	2.18	1.36
Stickleback back-transformed LSmean [MeHg] (μg/g)	0.09	0.21	0.09	0.26	0.11	0.20
Macroinvertebrate mean [MeHg] (ng/g dry weight)	50.58	35.66	50.72	39.64	37.97	26.86
Bulk Zooplankton [MeHg] (ng/g dry weight)	14.69	13.16	13.44	4.66	16.31	12.13
Estimated submerged macrophyte cover (%)	10–25	<10	<10	75–90	75–90	90–100

3.2. Total mercury and methylmercury in water, sediment and periphyton

As the more catchment-influenced RDC lakes had higher SUVA and DOC concentrations, higher concentrations of Hg in the water and sediment of RDC lakes were expected, based on the findings of other studies linking Hg and allochthonous organic matter delivery in catchment runoff (Isidorova et al., 2016; Bravo et al., 2017). Despite the differences in inferred catchment connectivity discussed above, there were no significant differences between regions in concentrations of total Hg (t-test, $t = 1.44$, $p = 0.29$, df = 2.02) or MeHg (t-test, $t = 1.20$, $p = 0.35$, df = 2.0) in unfiltered water samples, or in concentrations of total Hg in filtered water samples (t-test, $t = 0.90$, $p = 0.42$, df = 4) (see Table S4 for statistical power, however). There were also no significant differences between regions in THg in sediment (t-test; $t = 2.03$, $p = 0.11$, df = 4; Fig. 3) or periphyton (t-test; $t = 1.06$, p = 0.35, df = 4; Fig. 3). Concentrations of MeHg in filtered water could not be statistically compared between regions because several values were less than the method detection limit (MDL = 0.006 ng/L).

In contrast with water and sediment THg results, significant differences were detected between regions for [MeHg] and %MeHg in sediment. Percent MeHg (of total Hg) can be used as a proxy for net methylation rates, such that a higher %MeHg indicates higher net methylation (Benoit et al., 2003; Drott et al., 2007; Drott et al., 2008). Mean [MeHg] and %MeHg in sediment were significantly higher in the ATQ region than in the RDC region (t-tests; $t > 8.56$, $p < 0.01$, df > 2.02; Fig. 3). Higher inferred MeHg production in sediments of the ATQ lakes are likely a product of greater autochthonous primary production, as algal-derived organic matter has been linked to higher Hg methylation rates in lake (Bravo et al., 2017), estuarine (Drott et al., 2007), and marine sediments (Kim et al., 2011) due to greater bioavailability. A future analysis of organic carbon quality and quantity in sediment could be used to test this assertion.

Mean [MeHg] and %MeHg in periphyton also differed significantly between regions but the pattern was reversed, with significantly higher values in the RDC region than in the ATQ region (t-tests; $t > 2.79$, $p < 0.05$, df = 4; Fig. 3), suggesting that MeHg production in littoral periphyton and associated biofilms was higher in the more allochthonous RDC lakes (Fig. 3). In the RDC lakes, %MeHg was significantly higher in periphyton than in sediments (Paired t-test; $t = 12.77$, $p < 0.01$, df = 2; Fig. 3), indicating that periphyton and associated biofilms were likely more important sites of Hg methylation than sediments. Although Hg methylation is conventionally thought to occur primarily in anoxic sediment porewaters (e.g., Gilmour et al., 1992), periphyton on beds of macrophytes provide an ideal environment for biofilms that include sulphate reducing bacteria, and can be Hg methylation "hot spots" (Mauro et al., 2001; Hamelin et al., 2011). Results from several studies on waterbodies in Brazil (Mauro et al., 2001; Achá et al., 2012), Florida (Mauro et al., 2002), and Wisconsin (Mauro et al., 2002) have indicated that MeHg production is elevated in periphyton associated with macrophyte beds. In this study, not only was periphyton far more abundant by visual observation in the RDC lakes due to greater macrophyte cover

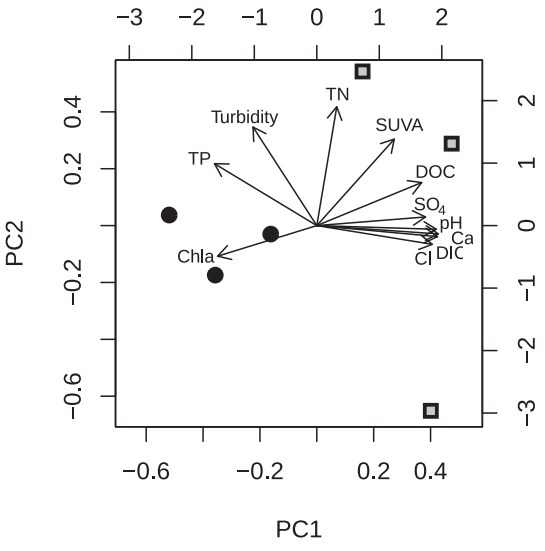

Fig. 2. Biplot of a principal components analysis for water chemistry data on the six study lakes; Atqasuk (ATQ) lakes are represented with circles and Reindeer Camp (RDC) lakes are represented with squares; ATQ lakes have more negative loadings on PC1, and are associated with indicators of higher autochthonous production whereas RDC lakes have more positive loadings, and are associated with indicators of catchment inputs.

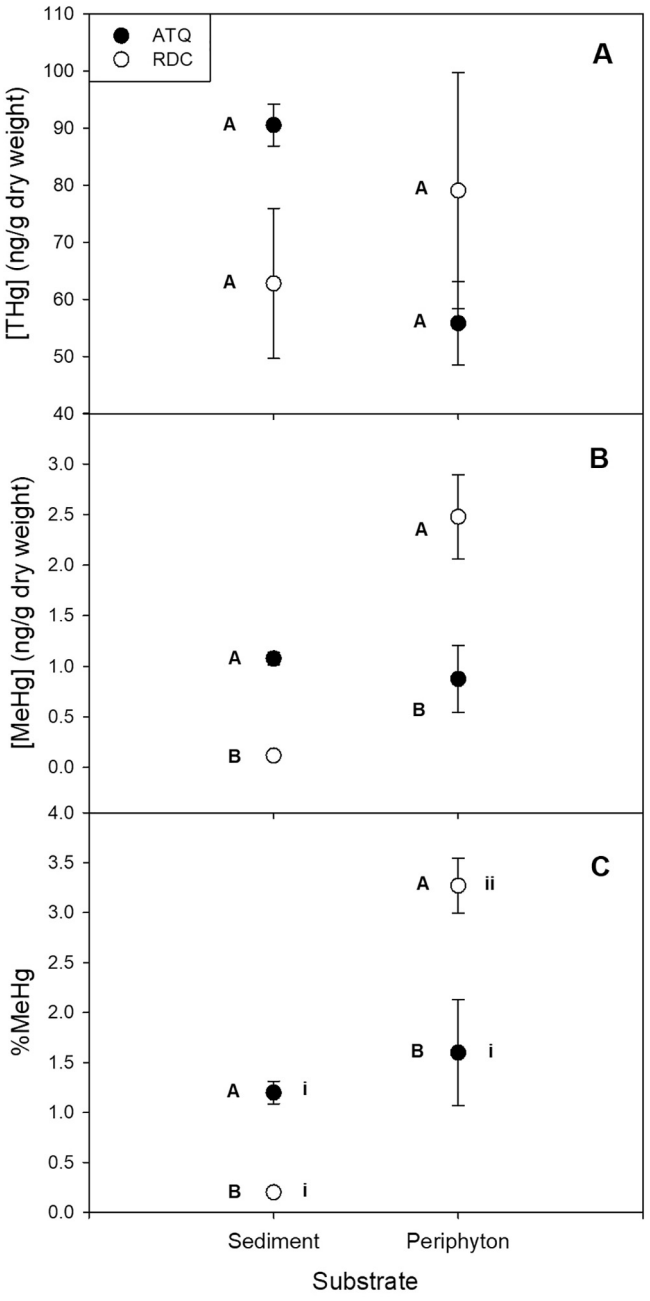

Fig. 3. Mean ± SE of mean total mercury concentrations (A), methylmercury concentrations (B), and %MeHg (C) in sediment and periphyton for each of the two regions. Information about regional means is located in Table S2. Filled circles represent Atqasuk (ATQ) lakes, and open circles represent Reindeer Camp (RDC) lakes. Significant differences between regions are indicated by different letters, whereas significant differences between substrates (i.e., sediment and periphyton) and within regions are indicated by different roman numerals.

(Table 1), but periphyton in the RDC lakes received relatively greater inputs of SO_4 (Table 1), the terminal electron acceptor for SO_4 reduction by sulphate-reducing bacteria - principal methylators in freshwater systems (Gilmour et al., 1992; Branfireun et al., 1999). Whereas %MeHg in sediment was negatively correlated with indicators of catchment-derived inputs, such as SO_4, Cl, and DOC (Table S6), %MeHg in periphyton was positively correlated with both SO_4 and Cl (Table S6). Lake water SO_4 explained >75% of the variability in %MeHg in periphyton among lakes (Linear regression, $R^2_{adj} = 0.77$, $F_{(1,4)=}17.75$, $p = 0.01$; Fig. 4), further supporting the link between SO_4 and Hg methylation. Although SO_4 reduction and Hg methylation were not measured directly as part of this work, the clarity of the relationship points toward a mechanistic link. Moreover, the SO_4 concentrations measured were much lower than concentrations that have been found to cause sulfide-induced inhibition of methylation in systems at lower latitudes (Gilmour et al., 1992; Gabriel et al., 2014).

3.3. Methylmercury in zooplankton, invertebrates and fish

A comparison of mean [MeHg] in bulk zooplankton found no differences between regions (*t*-test, $t = 0.79$, $p = 0.51$, df = 2.08; Table 1), despite differences in [MeHg] in sediment and periphyton. This finding may be the result of using bulk plankton samples (i.e. phytoplankton not removed), rather than a true lack of a relationship among lakes or between regions. Methylmercury in bulk zooplankton samples from the ATQ lakes could have been diluted by abundant phytoplankton, which are relatively lower in MeHg, and which were analyzed together with zooplankton (i.e., seston). Other authors have concluded that certain zooplankton taxa (i.e., *Daphnia* spp.) have higher [MeHg] because they are more efficient grazers than others (Chetelat and Amyot, 2009). In a companion study that included the same lakes reported on here, Guernon (2019) compared [MeHg] among bulk zooplankton, live-sorted Cladocera and live-sorted Copepoda. Cladocera had higher [MeHg] than either Copepoda or bulk zooplankton in the more autochthonous ATQ lakes, whereas Copepoda had higher [MeHg] than either Cladocera or bulk zooplankton in the more allochthonous RDC lakes (Guernon, 2019). These results could be driven by between-region differences in basal carbon sources (e.g., bacteria vs. algae) and/or feeding strategies in zooplankton taxa. Higher [MeHg] in Cladocera (a grazer) in the ATQ lakes is consistent with higher sediment [MeHg] in the more autochthonous lakes. Similarly, higher [MeHg] in Copopoda in the RDC lakes is consistent with their feeding in and on biofilms with higher MeHg; various copepod taxa have been found to be benthic-dwelling and reliant on bacterial/detrital carbon pathways (e.g., Perlmutter and Meyer, 1991; Reiss and Schmid-Araya, 2011). Bulk zooplankton samples were analyzed for their stable carbon isotope ratios, as more depleted ratios in the RDC lakes relative to the ATQ lakes would suggest a greater relative importance of bacterial-based production in the RDC lakes. There was no statistically significant difference in $\delta^{13}C$ of bulk zooplankton between the regions (*t*-test, $t = 1.38$, $p = 0.24$, df = 4; Fig. 4; Table S4); however, this could be a function of both the mixed nature of the bulk samples, as well as low statistical power (Table S4).

There was no difference between regions in overall mean [MeHg] calculated for all benthic macroinvertebrates captured in each lake (see Table S5) (*t*-test, $t = 1.69$, $p = 0.17$, df = 4; Table 1). This analysis did not consider among-lake or between-region differences in community composition or relative abundance of functional feeding groups, however Sphaeridae (fingernail clam), Chironomidae (non-carnivorous midge larvae), and Tanypodinae (carnivorous midge larvae) were found in every lake at high enough abundances to allow taxa-specific comparisons of [MeHg]. Mean [MeHg] in filter-feeding Sphaeridae was significantly higher in autochthonous ATQ lakes than in the allochthonous RDC lakes, which is consistent with the higher MeHg concentrations in the sediments of the ATQ lakes (*t*-test, $t = 2.45$, $p = 0.04$, df = 4, Fig. S1). There were no significant regional differences in [MeHg] in either Chironomidae (collector-gatherers) or Tanypodinae (predator-engulfers) (*t*-tests, $t < 0.31$, $p > 0.25$, $2.79 <$ df = 4; Fig. S1). This could reflect the fact that both of these taxa can live and feed in either sediment porewaters (higher MeHg in ATQ) or biofilm (higher in MeHg in RDC; Merritt and Cummins, 1996), and individuals were aggregated from both of these environments to achieve the biomasses necessary for mercury analysis.

Despite the a priori regional lake classification and the physicochemical data that supported it as part of this work, there was no overall pattern or significant difference in stickleback LSmean [MeHg] between regions (*t*-test, $t = 1.05$, $p = 0.35$, df = 4; Fig. 5). One ATQ lake (ATQ 201) had stickleback with relatively high [MeHg] compared to the other two ATQ lakes, whereas one RDC lake (RDC 309) had stickleback with relatively low [MeHg] compared to the other two RDC lakes. To evaluate the driver(s) of among-lake variability in LSmean [MeHg] in stickleback (at the mean length of 50 mm), relevant biotic and abiotic covariates were related to LSmean stickleback [MeHg] using Pearson's product-moment correlation (Table S7). We expected that [MeHg] in fish would be related to variables that indicate allochthonous vs.

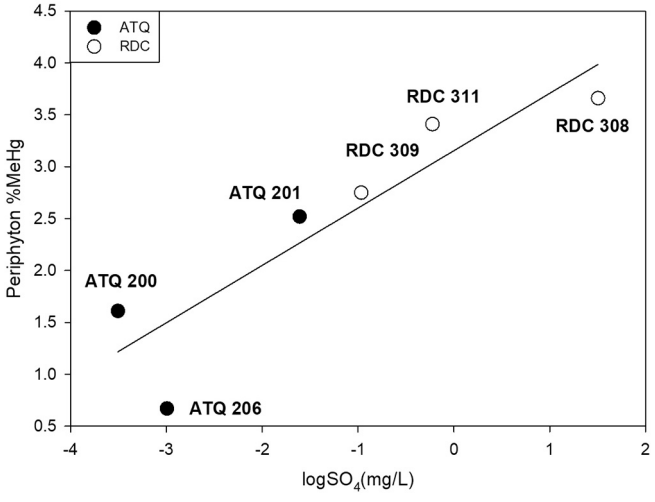

Fig. 4. Percent MeHg in periphyton related to log[SO_4] for each study lake on the Arctic Coastal Plain of Alaska; filled circles represent Atqasuk (ATQ) lakes, and open circles represent Reindeer Camp (RDC) lakes. There was a significant and positive relationship between %MeHg in periphyton and log[SO_4] (Linear regression, $R^2_{adj} = 0.77$, $F_{(1,4)} = 17.75$, $p = 0.01$).

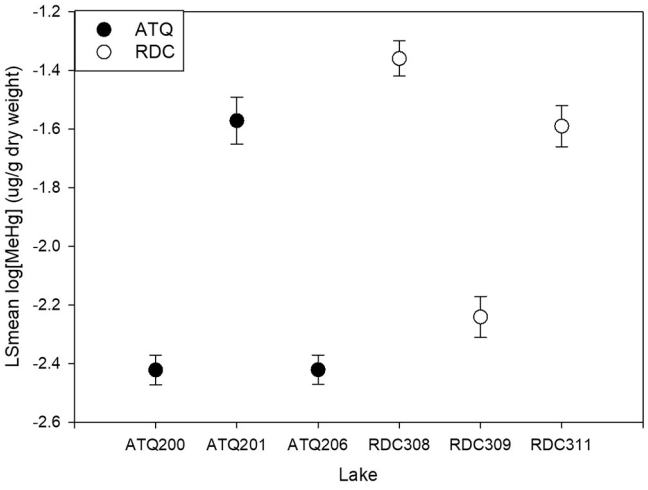

Fig. 5. Least-squares mean log[MeHg] in stickleback ± SE (μg/g dry weight) calculated at a size of 50 mm in each of the six study lakes. Filled circles represent Atqasuk (ATQ) lakes, and open circles represent Reindeer Camp (RDC) lakes.

autochthonous primary production, but neither DOC nor Chl-*a* concentrations were significantly correlated to LSmean [MeHg] in stickleback (Table S7). However, lake-specific LSmean [MeHg] in stickleback was significantly and positively related to lake water SO_4 and lake-specific LSmean stickleback age (at 50 mm total length) (Table S7), and a multiple regression with both of these variables accounted for 94% of the among-lake variability in length-adjusted mean [MeHg] in stickleback ($R^2_{adj} = 0.94$, $F_{(2,3)} = 41.87$, $p = 0.006$; Fig. 6).

The significant positive relationship between lake water SO_4 and length-adjusted mean MeHg concentration in stickleback could reflect higher net methylation rates in lakes with higher SO_4 (Gabriel et al., 2014), however, there were no consistent differences among lakes in [MeHg] in primary consumers (macroinvertebrates and zooplankton), which would be expected if the effect of SO_4 on fish [Hg] was entirely driven by higher net methylation. There were also no relationships between [MeHg] in primary consumers and lake water SO_4 (Table S8); these relationships may be confounded by factors identified previously, as well as the single time point of sampling of lake water chemistry, which would be expected to be variable over time and influence the [MeHg] of shorter-lived organisms. In the Florida Everglades (Gabriel et al., 2014), the relationship between [MeHg] in fish and SO_4 was non-linear, but concentrations of Hg in fish were highest in waters with SO_4 concentrations ranging from 1 to 12 mg/L, a range that only the highest-sulphate lake in this study (RDC 308) falls within.

Whereas SO_4 acted as a regional abiotic driver for stickleback [MeHg], fish age-at-size (i.e., proxy for growth), was a significant biotic driver of fish [MeHg], and varied among lakes, but not systematically between regions. Fish age-at-size explained why stickleback from one of the lower sulfate lakes (ATQ 201) had higher [MeHg] (slower growth), whereas stickleback from one of the higher sulfate lakes (RDC 309) had lower [MeHg] (faster growth) (Fig. 6). The significant positive relationship between age-at-size and length-adjusted mean [MeHg] in ninespine stickleback indicated that the faster-growing fish had lower MeHg concentrations, which is consistent with somatic growth dilution (Karimi et al., 2007; Ward et al., 2010); faster growing organisms gain more biomass per unit food intake, which dilutes the MeHg burden in their tissues from the food they consume (e.g., Essington and Houser, 2003; Trudel and Rasmussen, 2006). This is most likely to happen when growth increases with minimal change in Hg consumption (e.g., high food quality; Karimi et al., 2007). Ninespine stickleback from the three lakes with the highest length-adjusted mean [MeHg] (RDC 311, RDC 308, and ATQ 201) were all older at the standardized length of 50 mm. Age-at-size has been found to predict Hg concentrations in several other Arctic fishes, including Arctic char (*Salvelinus alpinus*; Swanson and Kidd, 2010; Swanson et al., 2011) and lake trout (*Salvelinus namaycush*; Swanson et al., 2011).

Although the path between the supply of SO_4, net MeHg production, and ultimately bioaccumulation and food web biomagnification is complex, a conceptual understanding of the link between lake water SO_4 and fish [MeHg] in these lakes is informed by an examination of stable isotope ratios in biota from the two study regions. While $\delta^{13}C$ ratios of fish, macroinvertebrates, and bulk zooplankton in the ATQ lakes were indicative of a 'classic' pelagic signal (France, 1995), each of these taxa was more ^{13}C -depleted in the RDC lakes (Fig. 7). Both stickleback and benthic macroinvertebrates had significantly more negative $\delta^{13}C$ ratios in the RDC lakes compared to the ATQ lakes (*t*-tests, $t > 2.86$, $p \leq 0.05$, $df = 4$). Lower $\delta^{13}C$ values can be indicative of a more bacterial-based food web (Bunn and Boon, 1993), and suggest that the allochthonous RDC lakes support a detrital-based (biofilm) food web, whereas the autochthonous ATQ lakes support a grazing-based (algal) food web. Fatty acid analysis on all taxa would be helpful in further testing this assertion, and in interpreting results of MeHg analyses, because the extent to which a food web is phytoplankton- or bacterial-based has implications for mercury uptake and accumulation (e.g., de Wit et al., 2012; Poste et al., 2019). We posit that the relationship between lake water SO_4 and fish [MeHg] reflects not only differences in net rates and

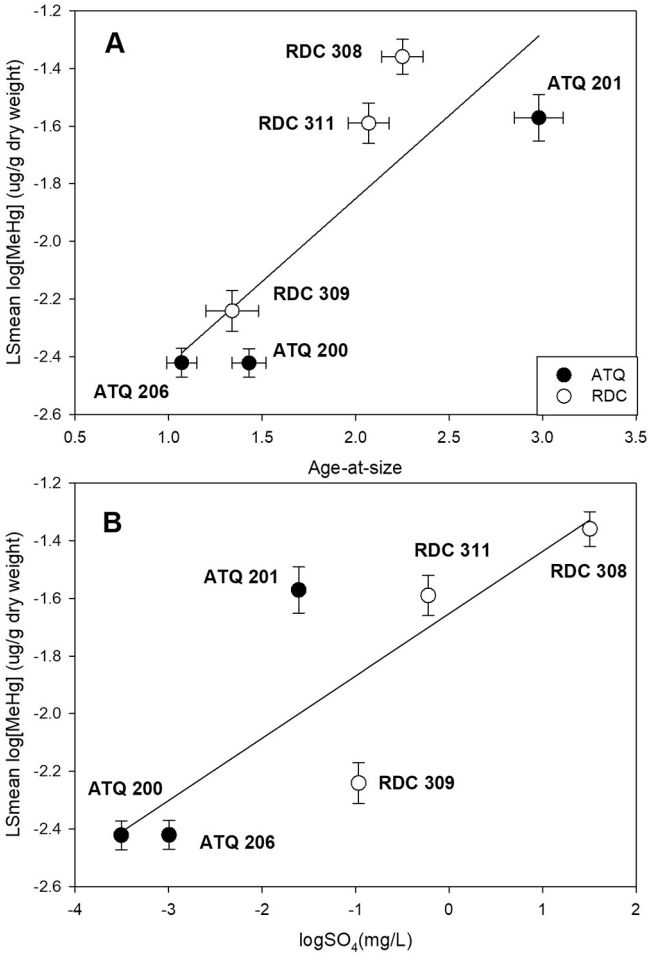

Fig. 6. Least squares mean [MeHg] in stickleback ± SE (μg/g dry weight) related to (A) least squares mean age-at-size (50 mm) and (B) log[SO_4] for each study lake. Filled circles represent Atqasuk (ATQ) lakes, and open circles represent Reindeer Camp (RDC) lakes.

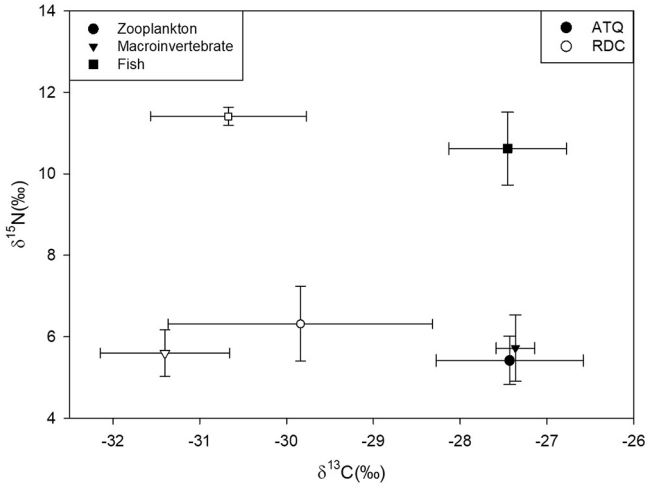

Fig. 7. Mean ± SE $\delta^{15}N$ and $\delta^{13}C$ for bulk zooplankton (circles), benthic macroinvertebrates (triangles), and whole body ninespine stickleback (squares). Stickleback ($p = 0.05$) and macroinvertebrates ($p = 0.02$) from the Reindeer Camp (RDC) lakes (open symbols) were significantly more ^{13}C-depleted than those in the Atqasuk (ATQ) lakes (filled symbols). Information about regional means is located in Table S3.

location of Hg methylation, but also catchment-mediated differences (traced by SO_4) in sources of production (bacterial vs. algal) and food availability for ninespine stickleback.

Crustacean zooplankton are preferred food items for stickleback; however, stickleback will consume less desirable prey (e.g., meiofauna) during times of food scarcity (Hynes, 1950; Laske et al., 2017). Abundance of crustacean zooplankton was lower in RDC lakes than in ATQ lakes (Guernon, 2019), which likely reflects regional differences in phytoplankton availability (Table 1; Fig. 2), or differences in predation pressure, which was not quantified. Low zooplankton availability in the RDC lakes may result in ninespine stickleback relying more on benthic macroinvertebrates than in the ATQ lakes. If true, this would result in higher MeHg exposure for ninespine stickleback in the RDC lakes, because benthic macroinvertebrates consistently had higher [MeHg] than zooplankton (Table 1). Both $\delta^{15}N$ and $\delta^{13}C$ ratios indicated that ninespine stickleback likely relied on both benthic and pelagic food sources in the study lakes (especially in the RDC lakes) (Fig. 7). Ideally, mixing model analysis would be used to determine and compare proportional contributions of zooplankton and benthic macroinvertebrates in stickleback diet for each lake and region; however, there was not enough isotopic separation between these two food sources to permit the analysis. Given the low abundance of zooplankton in the RDC lakes and the fact that benthic macroinvertebrates had higher [MeHg] than zooplankton in all lakes, stickleback were likely exposed to higher [MeHg] in diet in the RDC lakes, but this pattern of regionally higher exposure was complicated by variation in fish growth rates among lakes.

4. Summary and implications

Based on the literature, it was predicted that [MeHg] in all ecosystem components would be higher in the allochthonous RDC lakes than in the autochthonous ATQ lakes, and that DOC or Chl-*a* would best predict [MeHg] in ninespine stickleback. The relationship between fish Hg and environmental and ecological factors turned out to be far more complex and intriguing, however. Primary locations of Hg methylation (i.e., sediment porewaters in ATQ lakes, and periphyton in RDC lakes) and pathways of MeHg entry into the food web (i.e., via grazing food web in ATQ lakes, via biofilm-based food web in RDC lakes) differed between the two regions studied, and sources of primary production and food web ecology likely also differ between regions and among individual lakes.

This work, along with previous studies, indicates that greater catchment inputs and higher sedimentation rates in RDC lakes (Burke et al., 2018) has led to the development/persistence of extensive macrophyte beds with associated biofilms, which, combined with relatively high sulphate inputs from the catchment, facilitates higher Hg methylation rates in periphyton. The ATQ lakes were phytoplankton- rather than macrophyte-dominated, and the dominant location of Hg methylation was likely sediment porewaters. A combination of direct and indirect mechanisms explains the observed positive relationship between SO_4 and [MeHg] in ninespine stickleback. Sulphate stimulates net Hg methylation and is also a tracer of catchment inputs. Greater catchment influence promotes relatively higher abundance of macrophytes and periphyton, fewer zooplankton, and a consequently greater importance of benthic macroinvertebrates (with higher MeHg than zooplankton) in stickleback diets in these thermokarst lakes on the ACP.

Fish age-at-size, used as a proxy for lifetime average growth rates, was the strongest predictor of stickleback [MeHg], and variability in fish growth among individual lakes explained the lack of regional pattern in stickleback [MeHg]. Longer term monitoring of these or similar thermokarst lakes would allow better development and parameterization of models to predict the effects of climate change, as the ACP is a dynamic landscape that is experiencing a myriad of climate-related changes that affect catchment thermokarst activity (Grosse et al., 2013; Clow and Urban, 2002), aquatic chemistry and ecology (Hobbie et al., 2003; Koch et al., 2018a,b), and fish growth rates (Reist et al., 2006), all of which can affect Hg concentrations in fish. As such, the ability to elucidate and quantify dominant drivers of mercury accumulation at the landscape-level is critical to allowing more accurate predictions of how climate will impact mercury concentrations and accumulation in lakes in this region.

CRediT authorship contribution statement

S.M. Burke: Conceptualization, Methodology, Formal analysis, Investigation, Data curation, Writing - original draft, Writing - review & editing, Visualization. **C.E. Zimmerman:** Conceptualization, Methodology, Investigation, Resources, Writing - review & editing, Supervision, Project administration, Funding acquisition. **S.M. Laske:** Investigation, Resources, Data curation, Writing - review & editing, Visualization, Project administration. **J.C. Koch:** Conceptualization, Investigation, Writing - review & editing, Funding acquisition. **A.M. Derry:** Resources, Writing - review & editing, Supervision. **S. Guernon:** Investigation, Data curation, Writing - review & editing. **B.A. Branfireun:** Conceptualization, Methodology, Investigation, Resources, Data curation, Writing - original draft, Writing - review & editing. **H.K. Swanson:** Conceptualization, Methodology, Formal analysis, Investigation, Resources, Data curation, Writing - original draft, Writing - review & editing, Supervision, Project administration, Funding acquisition.

Declaration of competing interest

The authors declare that they have no known competing financial interests or personal relationships that could have appeared to influence the work reported in this paper.

Acknowledgements

We would like to acknowledge University of Alberta Biogeochemical Analytical Services Laboratory, Biotron Analytical Services at Western University, and Environmental Isotope Laboratory at the University of Waterloo for laboratory analyses. Dr. Leanne Baker, Amy Nguyen, Amanda Soliguin, Alexandra Crichton, and Daniel Donnelly provided field and laboratory assistance. We are very appreciative to the community of Atqasuk, AK for welcoming us during our field season. Symbols that were used in the graphical abstract were courtesy of the Integration and Application Network, University of Maryland Center for Environmental Science (ian.umces.edu/symbols/). S.M.B. was supported by scholarships from NSERC, the W. Garfield Weston Foundation, as well as by grants from the Northern Scientific Training Program (NSTP). The research was funded by the Arctic Landscape Conservation Cooperative (PI: C.E.Z.). Any use of trade, firm, or product names is for descriptive purposes only and does not imply endorsement by the U.S. Government.

Appendix A. Supplementary data

Supplementary data to this article can be found online at https://doi.org/10.1016/j.scitotenv.2020.140564.

References

Achá, D., Pabón, C.A., Hintelmann, H., 2012. Mercury methylation and hydrogen sulfide production among unexpected strains isolated from periphyton of two macrophytes of the Amazon. FEMS Microbiol. Ecol. 80 (3), 637–645.

Ahonen, S.A., Hayden, B., Leppänen, J.J., Kahilainen, K.K., 2018. Climate and productivity affect total mercury concentration and bioaccumulation rate of fish along a spatial gradient of subarctic lakes. Sci. Total Environ. 637–638, 1586–1596. https://doi.org/10.1016/j.scitotenv.2018.04.436.

Arctic Monitoring and Assessment Programme, 2011. Mercury in the Arctic. Arctic Monitoring and Assessment Programme (AMAP), Oslo, Norway xiv. 191 pp.

Benoit, J.M., Gilmour, C.C., Heyes, A., Mason, R.P., Miller, C.L., 2003. Geochemical and biological controls over methylmercury production and degradation in aquatic ecosystems. In: Chai, Y., Braids, O.C. (Eds.), Biogeochemistry of Environmentally Important Trace Elements, ACS Symposium Series #835. American Chemical Society, Washington, DC, pp. 262–297 2003.

Bloom, N., Fitzgerald, W.F., 1988. Determination of volatile mercury species at the picogram level by low-temperature gas chromatography with cold-vapour atomic fluorescence detection. Anal. Chim. Acta *208*, 151–161.

Bodaly, R.A., Rudd, J.W.M., Fudge, R.J.P., Kelly, C.A., 1993. Mercury concentrations in fish related to size of remote Canadian Shield lakes. Can. J. Fish. Aquat. Sci. 50 (5), 980–987.

Branfireun, B.A., Roulet, N.T., Kelly, C., Rudd, J.W., 1999. In situ sulphate stimulation of mercury methylation in a boreal peatland: toward a link between acid rain and methylmercury contamination in remote environments. Global. Biogeochem. Cy. 13 (3), 743–750.

Bravo, A.G., Bouchet, S., Tolu, J., Björn, E., Mateos-Rivera, A., Bertilsson, S., 2017. Molecular composition of organic matter controls methylmercury formation in boreal lakes. Nat. Commun. 8, 14255. https://doi.org/10.1038/ncomms14255.

Bunn, S.E., Boon, P.I., 1993. What sources of organic carbon drive food webs in billabongs? A study based on stable isotope analysis. Oecologia 96 (1), 85–94.

Burger, J., Stern, A.H., Gochfeld, M., 2004. Mercury in commercial fish: optimizing individual choices to reduce risk. Environ. Health. Persp. 113 (3), 266–271.

Burke, S.M., Zimmerman, C.E., Branfireun, B.A., Koch, J.C., Swanson, H.K., 2018. Patterns and controls of mercury accumulation in sediments from three thermokarst lakes on the Arctic Coastal Plain of Alaska. Aquat. Sci. 80 (1), 1.

Chetelat, J., Amyot, M., 2009. Elevated methylmercury in High Arctic Daphnia and the role of productivity in controlling their distribution. *Glob. Chang. Biol. 15* (3), 706–718.

Christophersen, N., Hooper, R.P., 1992. Multivariate analysis of stream water chemical data: the use of principal components analysis for the end-member mixing problem. Water Resour. Res. 28 (1), 99–107.

Clow, G.D., Urban, F.E., 2002, December. Large permafrost warming in northern Alaska during the 1990's determined from GTN-P borehole temperature measurements. AGU Fall Meeting Abstracts.

Compeau, G.C., Bartha, R., 1985. Sulfate-reducing bacteria: principal methylators of mercury in anoxic estuarine sediment. Appl. Environ. Microb. 50 (2), 498–502.

de Wit, H.A., Kainz, M.J., Lindholm, M., 2012. Methylmercury bioaccumulation in invertebrates of boreal streams in Norway: effects of aqueous methylmercury and diet retention. Environ. Pollut. 164, 235–241.

DeFaveri, J., Shikano, T., Merilä, J., 2014. Geographic variation in age structure and longevity in the nine-spined stickleback (*Pungitius pungitius*). PLoS One 9, e102660.

Deison, R., Smol, J.P., Kokelj, S.V., Pisaric, M.F., Kimpe, L.E., Poulain, A.J., ... Blais, J.M., 2012. Spatial and temporal assessment of mercury and organic matter in thermokarst affected lakes of the Mackenzie Delta Uplands, NT, Canada. Envir. Sci. Tech. 46 (16), 8748–8755.

Drott, A., Lambertsson, L., Björn, E., Skyllberg, U., 2007. Importance of dissolved neutral mercury sulfides for methyl mercury production in contaminated sediments. Envir. Sci. Tech. 41 (7), 2270–2276.

Drott, A., Lambertsson, L., Björn, E., Skyllberg, U., 2008. Do potential methylation rates reflect accumulated methyl mercury in contaminated sediments? Envir. Sci. Tech. 42 (1), 153–158.

Essington, T.E., Houser, J.N., 2003. The effect of whole-lake nutrient enrichment on mercury concentration in age-1 yellow perch. Trans. Am. Fish. Soc. 132 (1), 57–68.

Evers, D.C., Schmutz, J.A., Basu, N., DeSorbo, C.R., Fair, J., Gray, C.E., … & Wright, K.G. (2014). Historic and contemporary mercury exposure and potential risk to Yellow-billed Loons (Gavia adamsii) breeding in Alaska and Canada. Waterbirds, 37(1), 147–160.

Faul, F., Erdfelder, E., Lang, A.G., Buchner, A., 2007. G*Power 3: a flexible statistical power analysis program for the social, behavioral, and biomedical sciences. Behav. Res. Methods 39 (2), 175–191. https://doi.org/10.3758/bf03193146.

France, R.L., 1995. Differentiation between littoral and pelagic food webs in lakes using stable carbon isotopes. Limnol. Oceanogr. 40 (7), 1310–1313.

Frey, K., Sobczak, W., Mann, P., Holmes, R., 2016. Optical properties and bioavailability of dissolved organic matter along a flow-path continuum from soil pore waters to the Kolyma River mainstem, East Siberia. Biogeosciences 13 (8), 2279–2290.

Gabriel, M.C., Howard, N., Osborne, T.Z., 2014. Fish mercury and surface water sulfate relationships in the Everglades Protection Area. Environ. Manag. 53 (3), 583–593.

Gilmour, C.C., Henry, E.A., Mitchell, R., 1992. Sulfate stimulation of mercury methylation in freshwater sediments. Envir. Sci. Tech. 26 (11), 2281–2287.

Graham, A.M., Aiken, G.R., Gilmour, C.C., 2012. Dissolved organic matter enhances microbial mercury methylation under sulfidic conditions. Envir. Sci. Tech. 46 (5), 2715–2723.

Grosse, G., Jones, B., Arp, C., 2013. Thermokarst lakes, drainage, and drained basins. In: Schroder, J. (Ed.), Treatise on Geomorphology, Vol 8, Glacial and Periglacial Geomorphology. Academic Press, San Diego, pp. 325–353.

Guernon, S., 2019. The Role of Dissolved Organic Carbon and Zooplankton Community Composition on Methylmercury Bioaccumulation in Western Arctic Lakes. Master thesis. Université du Québec à Montréal, Master in Biology, Montréal (Québec, Canada).

Hamelin, S., Amyot, M., Barkay, T., Wang, Y., Planas, D., 2011. Methanogens: principal methylators of mercury in lake periphyton. Envir. Sci. Tech. 45 (18), 7693–7700.

Haynes, T.B., Rosenberger, A.E., Lindberg, M.S., Whitman, M., Schmutz, J.A., 2014. Patterns of lake occupancy by fish indicate different adaptations to life in a harsh Arctic environment. Freshw. Biol. 59 (9), 1884–1896.

Hinkel, Kenneth, 2013. Western Lake Water Hourly Time Series - Temperature, Depth, Dissolved Oxygen, Conductivity, Water Level (CALON). Urn:Node:ARCTIC. https://doi.org/10.18739/A2BV8X.

Hobbie, J.E., Shaver, G., Laundre, J., Slavik, K., Deegan, L., O'Brien, J., ... MacIntyre, S., 2003. Climate forcing at the arctic LTER site. Climate Variability and Ecosystem Response at Long-term Ecological Research (LTER) Sites. Oxford University Press, New York, pp. 74–91.

Hynes, H.B.N., 1950. The food of fresh-water sticklebacks (Gasterosteus aculeatus and Pygosteus pungitius), with a review of methods used in studies of the food of fishes. J.Anim. Ecol. 36–58.

Isidorova, A., Bravo, A.G., Riise, G., Bouchet, S., Björn, E., Sobek, S., 2016. The effect of lake browning and respiration mode on the burial and fate of carbon and mercury in the sediment of two boreal lakes. J. Geophys. Res. Biogeosci. 121 (1), 233–245.

Jones, J.W., Hynes, H.B.N., 1950. The age and growth of Gasterosteus aculeatus, Pygosteus pungitius and Spinachia vulgaris, as shown by their otoliths. J. Anim. Ecol. 19, 59–73.

Jorgenson, M.T., Grunblatt, J., 2013. Landscape-level ecological mapping of northern Alaska and field site photography. Report prepared for the Arctic Landscape Conservation Cooperative. Available at. http://arcticlcc.org/assets/products/ALCC2011-06/reports/NorthernAK_LandscapeMappping_Field_Photos_Final_RPT. pdf.

Kahilainen, K.K., Thomas, S.M., Keva, O., Hayden, B., Knudsen, R., Eloranta, A.P., Järvinen, A., 2016. Seasonal dietary shift to zooplankton influences stable isotope ratios and total mercury concentrations in Arctic charr (Salvelinus alpinus (L.)). Hydrobiologia 783 (1), 47–63. https://doi.org/10.1007/s10750-016-2685-y.

Kalff, J., 2001. Limnology: Inland Water Ecosystems. Prentice-Hall, New Jersey.

Karimi, R., Chen, C.Y., Pickhardt, P.C., Fisher, N.S., Folt, C.L., 2007. Stoichiometric controls of mercury dilution by growth. P. Natl. Acad. Sci 104 (18), 7477 7482.

Kidd, K.A., Hesslein, R.H., Fudge, R.J.P., Hallard, K.A., 1995. The influence of trophic level as measured by δ 15 N on mercury concentrations in freshwater organisms. Mercury as a Global Pollutant. Springer, Dordrecht, pp. 1011–1015.

Kidd, K., Clayden, M., Jardine, T., 2012. Bioaccumulation and biomagnification of mercury through food webs. Environmental Chemistry and Toxicology of Mercury. Wiley, Hoboken, pp. 455–499.

Kim, M., Han, S., Gieskes, J., Deheyn, D.D., 2011. Importance of organic matter lability for monomethylmercury production in sulfate-rich marine sediments. Sci. Total Environ. 409 (4), 778–784.

Koch, J.C., 2020. Descriptions, Depth to Refusal, and Field-saturated Hydraulic Conductivity of Soils on the Arctic Coastal Plain of Alaska, 2012–2016: U.S. Geological Survey Data Release. https://doi.org/10.5066/P9US8C5X.

Koch, J.C., Fondell, T.F., Laske, S., Schmutz, J.A., 2018a. Nutrient dynamics in partially drained arctic thaw lakes. J. Geophys. Res. Biogeosci. 123 (2), 440–452.

Koch, J.C., Jorgenson, M.T., Wickland, K.P., Kanevskiy, M., Striegl, R., 2018b. Ice wedge degradation and stabilization impact water budgets and nutrient cycling in Arctic trough ponds. J. Geophys. Res. Biogeosci. 123 (8), 2604–2616.

Kokelj, S.V., Zajdlik, B., Thompson, M.S., 2009. The impacts of thawing permafrost on the chemistry of lakes across the subarctic boreal-tundra transition, Mackenzie Delta region, Canada. Permafrost Periglac 20 (2), 185–199.

Korthals, E.T., Winfrey, M.R., 1987. Seasonal and spatial variations in mercury methylation and demethylation in an oligotrophic lake. Appl. Environ. Microbiol. 53 (10), 2397–2404.

Laske, S.M., Rosenberger, A.E., Kane, W.J., Wipfli, M.S., Zimmerman, C.E., 2017. Top-down control of invertebrates by Ninespine Stickleback in Arctic ponds. Freshw. Sci. 36 (1), 124–137. https://doi.org/10.1086/690675.

Laske, S.M., Rosenberger, A.E., Wipfli, M.S., Zimmerman, C.E., 2019. Surface water connectivity controls fish food web structure and complexity across local- and meta-food webs in Arctic Coastal Plain lakes. Food Webs 21, e00123. https://doi.org/10.1016/j.fooweb.2019.e00123.

Lehnherr, I., 2014. Methylmercury biogeochemistry: a review with special reference to Arctic aquatic ecosystems. Environ. Rev. 22 (3), 229–243.

Lenth, R.V., 2016. Least-squares means: the R package lsmeans. J. Stat. Softw. 69 (1), 1–33. https://doi.org/10.18637/jss.v069.i01.

Lockhart, W.L., Stern, G.A., Wagemann, R., Hunt, R.V., Metner, D.A., DeLaronde, J., ... Mount, K., 2005. Concentrations of mercury in tissues of beluga whales (Delphinapterus leucas) from several communities in the Canadian Arctic from 1981 to 2002. Sci. Total Environ 351, 391–412.

Mauro, J.B., Guimarães, J.R., Melamed, R., 2001. Mercury methylation in macrophyte roots of a tropical lake. Water Air Soil Pollut. 127 (1–4), 271–280.

Mauro, J., Guimaraes, J., Hintelmann, H., Watras, C., Haack, E., Coelho-Souza, S., 2002. Mercury methylation in macrophytes, periphyton, and water–comparative studies with stable and radio-mercury additions. Anal. Bioanal. Chem. 374 (6), 983–989.

Merritt, R.W., Cummins, K.W. (Eds.), 1996. An Introduction to the Aquatic Insects of North America. Kendall Hunt.

Mesquita, P.S., Wrona, F.J., Prowse, T.D., 2010. Effects of retrogressive permafrost thaw slumping on sediment chemistry and submerged macrophytes in Arctic tundra lakes. Freshw. Biol. 55 (11), 2347–2358.

Oksanen, J., Blanchet, F.G., Kindt, R., Legendre, P., Minchin, P. R., O'hara, R.B., … & Oksanen, M.J. (2013). Package 'vegan'. Community Ecology Package, Version, 2(9).

Outridge, P.M., Sanei, H., Stern, G.A., Hamilton, P.B., Goodarzi, F., 2007. Evidence for control of mercury accumulation rates in Canadian High Arctic lake sediments by variations of aquatic primary productivity. Environ. Sci. Technol. 41 (15), 5259–5265.

Paranjape, A.R., Hall, B.D., 2017. Recent advances in the study of mercury methylation in aquatic systems. Facets 2 (1), 85–119.

Perlmutter, D.G., Meyer, J.L., 1991. The impact of a stream-dwelling harpacticoid copepod upon detritally associated bacteria. Ecology 72 (6), 2170–2180.

Petrone, K.C., Jones, J.B., Hinzman, L.D., Boone, R.D., 2006. Seasonal export of carbon, nitrogen, and major solutes from Alaskan catchments with discontinuous permafrost. J. Geophys. Res. Biogeosci. 111 (G2).

Pickhardt, P.C., Folt, C.L., Chen, C.Y., Klaue, B., Blum, J.D., 2002. Algal blooms reduce the uptake of toxic methylmercury in freshwater food webs. P. Natl. Acad. Sci. 99 (7), 4419–4423.

Poste, A.E., Hoel, C.S., Andersen, T., Arts, M.T., Færøvig, P.J., Borgå, K., 2019. Terrestrial organic matter increases zooplankton methylmercury accumulation in a brown-water boreal lake. Sci. Total Environ. 674, 9–18.

QGIS Development Team, 2016. QGIS geographic information system. Open Source Geospatial Foundation Project.

Ravichandran, M., 2004. Interactions between mercury and dissolved organic matter––a review. Chemosphere 55 (3), 319–331.

Reiss, J., Schmid-Araya, J.M., 2011. Feeding response of a benthic copepod to ciliate prey type, prey concentration and habitat complexity. Freshw. Biol. 56 (8), 1519–1530.

Reist, J.D., Wrona, F.J., Prowse, T.D., Power, M., Dempson, J.B., King, J.R., Beamish, R.J., 2006. An overview of effects of climate change on selected Arctic freshwater and anadromous fishes. Ambio 35 (7), 381–388.

Rose, K.C., Williamson, C.E., Kissman, C.E., Saros, J.E., 2015. Does allochthony in lakes change across an elevation gradient? Ecology 96 (12), 3281–3291.

Sandheinrich, M.B., Drevnick, P.E., 2016. Relationship among mercury concentration, growth rate, and condition of northern pike: a tautology resolved? Environ. Toxicol. Chem. 35 (12), 2910–2915.

Scheuhammer, A.M., Basu, N., Burgess, N.M., Elliott, J.E., Campbell, G.D., Wayland, M., ... Rodrigue, J., 2008. Relationships among mercury, selenium, and neurochemical parameters in common loons (Gavia immer) and bald eagles (Haliaeetus leucocephalus). Ecotoxicology 17 (2), 93–101.

Schuster, P.F., Schaefer, K.M., Aiken, G.R., Antweiler, R.C., Dewild, J.F., Gryziec, J.D., ... Liu, L., 2018. Permafrost stores a globally significant amount of mercury. Geophys. Res. Lett. 45 (3), 1463–1471.

Scott, D.P., Armstrong, F.A.J., 1972. Mercury concentration in relation to size in several species of freshwater fishes from Manitoba and northwestern Ontario. J. Fish. Res. Board Can. 29 (12), 1685–1690.

Swanson, H.K., Kidd, K.A., 2010. Mercury concentrations in Arctic food fishes reflect the presence of anadromous Arctic charr (Salvelinus alpinus), species, and life history. Envir. Sci. Tech. 44 (9), 3286–3292.

Swanson, H., Gantner, N., Kidd, K.A., Muir, D.C.G., Reist, J.D., 2011. Comparison of mercury concentrations in landlocked, resident, and sea-run fish (Salvelinus spp.) from Nunavut, Canada. Environ. Toxicol. Chem. 30 (6), 1459–1467.

Thienpont, J.R., Ruehland, K.M., Pisaric, M.F., Kokelj, S.V., Kimpe, L.E., Blais, J.M., Smol, J.P., 2013. Biological responses to permafrost thaw slumping in Canadian Arctic lakes. Freshw. Biol. 58 (2), 337–353.

Thompson, M.S., Kokelj, S.V., Prowse, T.D., Wrona, F.J., 2008. The impact of sediments derived from thawing permafrost on tundra lake water chemistry: An experimental approach. In: Kane, D.L., Hinkel, K.M. (Eds.), Proceedings of the 9th International Conference on Permafrost. vol. 2, pp. 1763–1768 June.

Trudel, M., Rasmussen, J.B., 2006. Bioenergetics and mercury dynamics in fish: a modelling perspective. Can. J. Fish. Aquat. Sci. 63 (8), 1890–1902.

U.S. Environmental Protection Agency (EPA), 1996. Method 1669 sampling ambient water for trace metals at EPA water quality criteria levels. https://www.epa.gov/sites/production/files/201510/documents/method_1669_1996.pdf.

U.S. Environmental Protection Agency (EPA), 1998. Method 1630 methyl mercury in water by distillation, aqueous ethylation, purge and trap, and cold vapor atomic fluorescence spectrometry. https://www.epa.gov/sites/production/files/2015-08/documents/method_1630_1998.pdf.

Ward, D.M., Nislow, K.H., Chen, C.Y., Folt, C.L., 2010. Rapid, efficient growth reduces mercury concentrations in stream-dwelling Atlantic salmon. Trans. Am. Fish. Soc. 139 (1), 1–10.

Watras, C.J., Morrison, K.A., Host, J.S., Bloom, N.S., 1995. Concentration of mercury species in relationship to other site-specific factors in the surface waters of northern Wisconsin lakes. Limnol. Oceanogr. 40 (3), 556 565.

Weishaar, J.L., Aiken, G.R., Bergamaschi, B.A., Fram, M.S., Fujii, R., Mopper, K., 2003. Evaluation of specific ultraviolet absorbance as an indicator of the chemical composition and reactivity of dissolved organic carbon. Envir. Sci. Tech. 37 (20), 4702–4708.